A major purpose of the Technical Information Center is to provide the broadest dissemination possible of information contained in DOE's Research and Development Reports to business, industry, the academic community, and federal, state and local governments.

Although a small portion of this report is not reproducible, it is being made available to expedite the availability of information on the research discussed herein.

1

CONF-830911--31

LA-UR--83-2622

DE84 001344

Los Alamos National Laboratory is operated by the University of California for the United States Department of Energy under contract W-7405-ENG-36.

TITLE: PULSED-POWER Diode GENERATION OF HIGH-POWER MICROWAVES

AUTHOR(S): Anthony L. Peratt, Michael A. Mostrom, Thomas J. T. Kwan, and Lester E. Thode

SUBMITTED TO: Fifth International Topical Conference on High-Power Electron and Ion-Beam Research and Technology

September 12-14, 1983
San Francisco, CA

Los Alamos Los Alamos National Laboratory
Los Alamos, New Mexico 87545

PULSED-POWER DIODE GENERATION OF HIGH-POWER MICROWAVES

A. L. Peratt, M. A. Mostrom, T. J. T. Kwan, and L. E. Thode
Advanced Concepts and Plasma Applications Group
Los Alamos National Laboratory
Los Alamos, New Mexico 87545

Abstract

The generation of microwave radiation at gigahertz frequencies in high-voltage pulsed-power diodes has been investigated with electromagnetic particle simulations. Pulsed power in the form of a 0.5-1.0 MV, TEM wave is fed to the diode via a 5-cm diameter cylindrical stalk onto which a 30-cm diameter cathode has been mounted. Located some 3-5 cm in front of the cathode is a foil anode grid.

As the TEM wave propagates between the stalk and an outer cylindrical cage (70-cm diameter) a stream of electrons are emitted off the stalk when the local electric field exceeds 200 kV/cm. This flow is then magnetically insulated and confined by the induced B_θ fields resulting from the 25-50-kA current flow within the stalk. Convex shaping of the cathode surface allows the emitted electrons to form a virtual cathode beyond the grid, then phase bunch to produce narrow bandwidth 1-GHz microwaves over an area equal to that of the cathode. The electromagnetic radiation from the dipole-like electron motions centered on the grid, which follow closely the classical Barkhausen-Kurz description, are reported.

Introduction

The development of high-current, pulsed-power accelerators has spurred interest in the use of intense relativistic electron beams to produce microwaves. Electron beams at multi-terawatt power levels and mega-electron-volt energies make it possible to raise the power of electronic microwave devices by several orders of magnitude. One mechanism by which ultra-high-power microwaves may be produced in a pulsed-power generator is the formation of a reflecting electron system. The advantages of a reflecting electron system include: emitted power maxima in the absence of external guide magnetic fields, monochromaticity, tunability, and configuration simplicity.

In its simplest form, a reflecting electron system consists of a cathode and a semi-transparent grid/anode. Electrons emitted from the cathode are accelerated by a voltage pulse applied to the anode-cathode gap, pass through the grid/anode, and form a virtual cathode. As a result of the positive potential on the anode, electrons reflected by the virtual cathode are accelerated back through the anode and then oscillate between the real and virtual cathodes. The mechanism described above was first utilized and described by Barkhausen and Kurz to produce low-power centimeter waves as early as 1920 [1].

More recently, power levels approaching 100 MW at frequencies in the range 2-13 GHz, with electron beam power conversion efficiencies between 1.5 and 12%, have been reported from experiments utilizing low impedance pulsed-power generators [2-5].

2½-D Electromagnetic Particle Simulations

The system under investigation concerns the modeling of a 13-cm radius, convex face cathode spaced 3-5 cm away from a transparent anode. A 750-kV to 1-MV pulse is applied to this diode configuration at time zero in the form of a TEM wave launched into a coaxial vacuum chamber. Figure 1 illustrates geometry under consideration. Azimuthal symmetry is assumed for the sequence of events described below. The computer code used here is CCUBE, a 2½-dimensional, relativistic PIC code [6].

The launched TEM wave (triangular-shaped in time) enters the left-hand aperture and propagates within a vacuum region defined by an outer conducting boundary of radius 35-cm and an inner conducting rod (stalk) of radius 2.5 cm. Electrons emit off the cathode stalk whenever the local electric field strength on any part of the inner (cathode) boundary exceeds 200 kV/cm. A stress region for electron emission occurs near the left-hand aperture at early times and continues to supply electrons during the course of the simulation. At time t = 3.2 ns, the cathode face begins to emit electrons in increasing numbers, as illustrated in the subsequent time frames of Fig. 1. (The "light-up" and emission of the cathode is more uniform than indicated in this figure as only the electrons coming off every third simulation vertex point, along the cathode surface, are plotted.)

For times greater than 1.6 ns, a conducting path through the outer wall-anode-cathode allows the electrical current flow through the cathode stalk to establish a magnetic blanket around this rod from the self-induced azimuthal field. The subsequent electron emission from stress regions near the aperture are confined to the stalk region as a result of the magnetic insulation.

The field-emitted cathode electrons are accelerated through the anode then bunch up to form a virtual cathode cloud beyond the anode. The virtual cathode is formed at a distance slightly greater than the anode-cathode gap spacing beyond the anode. The virtual cathode formation is determined by the space charge limiting current parameter.

The space charge limiting current for a solid beam within a conducting cylinder is given by [7]

$$I_{SC} = \frac{17\ kA(\gamma^{2/3} - 1)^{3/2}}{1 + 2\ \ln(R/a)} , \qquad (1)$$

where $\gamma = (1 - \beta^2)^{-1/2}$, $\beta = v/c$ for electrons with velocity v, R = 22.6 cm is the boundary radius beyond the anode, and a is the radius of the relativistic electron beam. For a 1-MeV cathode emitted electron beam whose approximate radius is 10 cm, I_{SC} = 7.4 kA. This value is an estimate based upon the assumptions of a uniformly solid electron beam forming a virtual cathode layer within a coaxial outer conductor. In the simulation figures (Fig. 1), the electron beam emitted off the cathode is neither entirely uniform nor solid. Additionally, a fraction of the electron flow is bled off by the outer conducting walls beyond the virtual cathode. Because of this, Rogowski coil and Faraday cup simulation diagnostics yield diode currents somewhat higher than I_{SC}. A diode current of 27 kA is measured in the simulation pertaining to Fig. 1.

Figure 2 illustrates the phase-space sequence of the reflecting system. At time t = 3.2 ns the electrons have reached a maximum velocity at the anode then, after having passed through the anode, begin to decelerate. At t = 4.8 ns, the virtual cathode has started to form and a number of electrons are reflected back into the anode. More energetic electrons escape the system through the open right-hand boundary. Those electrons trapped within the potential trough centered on the anode undergo oscillations at an average cycle time of about 0.66 ns. These oscillations are well-established by a time 8 ns after pulse launching.

In addition to the cyclic phase behavior depicted in Fig. 2, the virtual cathode also oscillates with a "whip-like" motion (the inward cloud

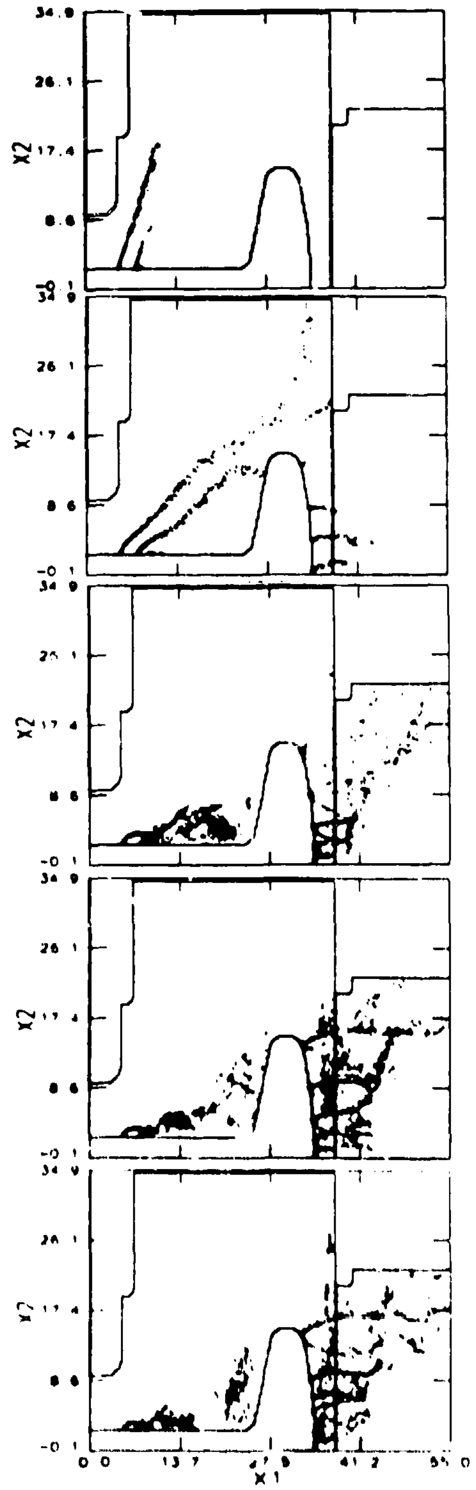

Fig. 1. Configuration space sequence of reflecting electron system. The figures are azimuthally symmetric about the horizontal axis. The frames illustrated correspond to times of 1.6, 3.2, 4.8, 6.4, and 8.0 ns, respectively. The vertical and horizontal axes are calibrated in centimeters. This data corresponds to a 1-MV pulse and a 3-cm gap

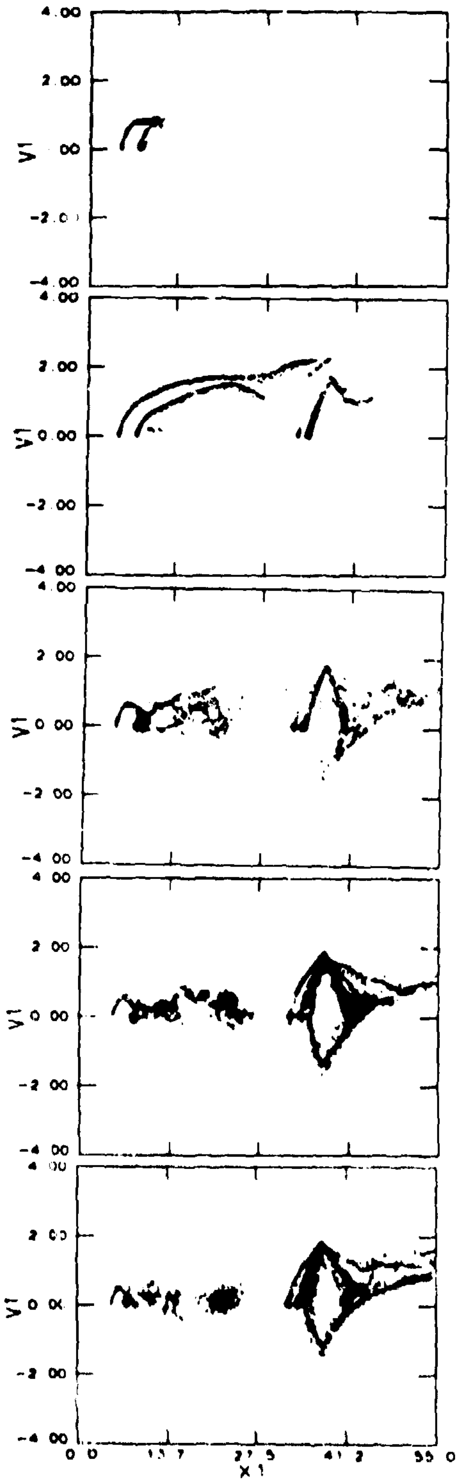

Fig. 2. Phase-space sequence of the formation of reflexing electrons between cathode and virtual cathode. Same parameters as Fig. 1. The ordinate is given in units of $\gamma\beta$.

displacement is much more rapid then the outward cloud displacement along the horizontal axis). However, for this configuration, the radiation from the virtual cathode oscillations is weak relative to the reflexing electron source.

The microwave radiation and poynting flux from the nearly axial oscillating electrons are recorded by both radial electric field an azimuthal magnetic field probes that are located throughout the entire simulation region. The azimuthal magnetic field measured by a probe located 6 cm off axis at the right-hand boundary is shown in Fig. 3a. A Fourier analysis of the temporal behavior of this field is illustrated in Fig. 3b. The radiation emitted during this simulation was primarily at 1.52 GHz.

Additional simulations were run for a variety of pulse amplitudes and gap spacings. The radiation frequency dependency versus the square root of the voltage pulse is given in Fig. 4 for an anode-cathode gap of 3 cm. Not shown is the frequency dependency of the relatively weak radiation when the pulse voltage was less than 1 MV for a 5-cm gap. Also shown in Fig. 4 are the experimental measurements of Mahaffey, et al who reported a frequency dependency $f \sim V^{1/2}/D^{n}$, where V is the anode voltage, D is the cathode-virtual-cathode spacing, and n is a number $0 < n \leq 1$ [2]. The diode geometry consisted of a 8.4-cm solid flat-faced carbon cathode spaced 0.8-1.6 cm from a transparent anode to which a 50-ns, 250-350-kV pulse was applied.

The striking feature of the experimental results shown in Fig. 4 is the variation of microwave frequency with applied voltage. Additionally, it has been reported that the frequency depends on the shape of the cathode [2] or anode [3]. The simulation

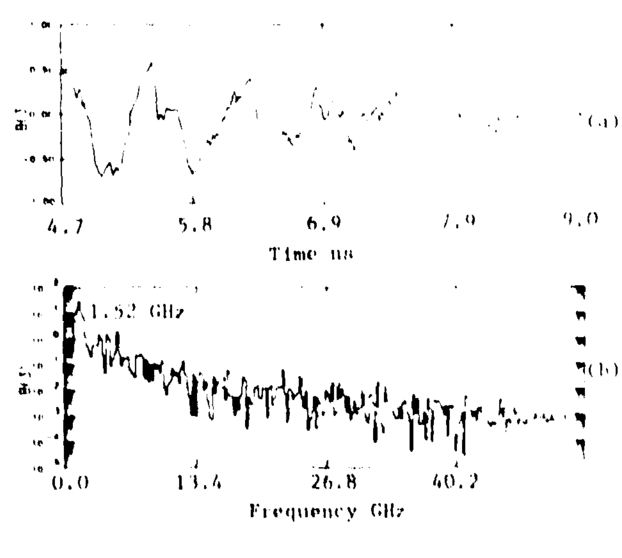

Fig. 3. Time variation and frequency spectrum of the azimuthal magnetic field measured at the middle, right-hand-side boundary of the simulation region. The amplitude of the field is given in units of ω_c/ω_p.

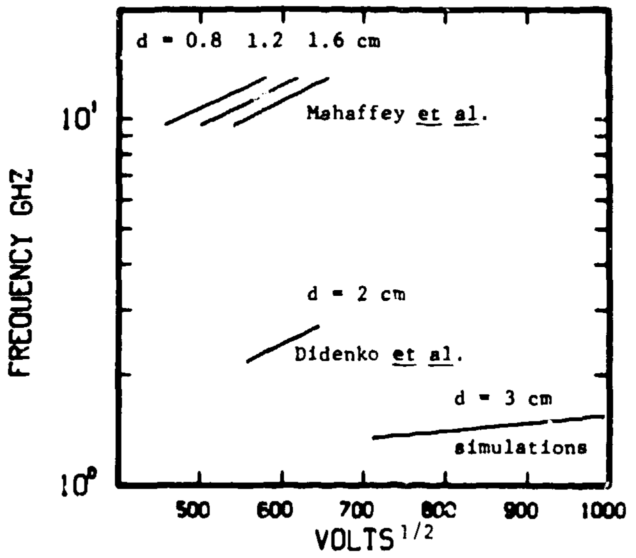

Fig. 4. Average frequency vs. the square root of the applied voltage for three experimental anode-cathode spacings and one simulation spacing.

results agree with this behavior although the frequency-voltage dependency is weaker than that found in the lower voltage experimental situations [2-3]. We have also simulated different cathode shapes and wider (to 35 cm) outer boundary radii beyond the anode. Frequencies as high as 3 GHz were observed with these variations.

The impedance of the diode was measured by placing voltage/current probes along the outer boundaries of the simulation region. While the time-varying impedance tended to be spikey, a result of the complex diode power flow and emission characteristics, the average impedance was abou 25 Ω.

Conclusions

A 2½-dimensional, electromagnetic PIC treatment of a reflecting electron system in a pulsed-power generator has been carried out to study the production of ultra-high power microwaves. The system utilizes magnetic-insulation in the process of delivering energy to the cathode-transparent-anode diode. Radiation from electrons trapped with a megavolt potential well of approximately 6 cm total extent is observed at 1.52 GHz. The simulation results reported here are in apparent agreement with earlier reported high-power microwaves from a closely related experimental setup. In particular, a frequency dependency on the applied voltage and anode-cathode gap is measured, as well as a frequency variation due to the diode shape. Simulation improvements presently under study include the effects of electron scattering from the anode and the closure of the diode region due to inflowing plasma.

Acknowledgments

The authors acknowledge discussions with B. Freeman and R. Hoberling. We also acknowledge the efforts of J. Lunsford and C. Snell on maintaining and upgrading the code CCUBE.

This work is supported by the U.S. Department of Energy.

References

1. V. H. Burkhausen and K. Kurz, Physik. Zeit. 21, 1 (1920).

2. R. A. Mahaffey, P. Sprangle, J. Golden, and C. A. Kapetanakos, Phys. Rev. Lett. 39, 843 (1977).

3. A. N Didenko, Ya. E. Krasik, S. F. Perlygin, and G. P. Fomenko, Sov. Tech. Phys. Lett. 5, 128 (1979).

4. H. E. Brandt, A. Bromborsky, H. B. Bruns, and R. A. Kehns, Proceedings of the 2nd International Topical Conference on High Power Electron and Ion Beam Research and Technology (October 3-5, 1977, Ithaca, New York) p. 649.

5. J. M. Buzzi, H. J. Doucet B. Etlicher, P. Haldenwang, A. Huetz, H. Lamain, C. Rouille, J. Cabe, J. Delvaux, J. C. Jouys, and C. Pe gnet, loc. cit., p. 663.

6. M. M. Campbell, D. J. Sullivan, and B. B. Godfrey, Mission Research Corporation report AMRC-R-341 (1982).

7. L. S. Bogdankevich and A. A. Rukhadze, Sov. Phys Usp. 14, 163 (1971).